THERMAL MODE OF A RESISTANCE FURNACE FOR DRAWING OPTICAL FIBER.
I. GENERALIZED MATHEMATICAL MODEL OF THE HEATING UNIT

V. N. Vasil'ev, G. N. Dul'nev, and V. D. Naumchik UDC 621.365.3

A foundation is given for a physical and mathematical model of a resistance furnace for drawing optical fibers and the algorithm for the numerical solutions of the problem formulated is considered.

It is known that the quality of fibers depends substantially on the temperature mode of the drawing, which is determined by the heating unit for preparation at the required temperature. Graphite resistance furnaces [1] are used extensively in recent years for the fabrication of high-quality quartz optical fibers, where the design is, as a rule, performed at an empirical level without a total analysis of the thermal mode.

The thermal mode of a resistance furnace is investigated below and methods to assure the most favorable temperature conditions for fiber formation as well as an increase in the lifetime of the graphite heating element are discussed.

On the basis of an analysis of the structural features of the main types of resistance furnaces [2-4] utilized for the industrial production of optical fiber, a thermal model was developed for the heating unit which includes the housing 1 with graphite heating element 2 (Fig. 1) which is a hollow cylinder with variable outer and inner diameters. Thermal insulation is provided from the outside and inside of the heater by using the cylindrical screens 3 and 4. The mathematical model of the heating unit should permit determination of the temperature field of the graphite heating element as a function of the structural features of the furnace and the fiber formation conditions. It is hence assumed that the temperature distribution in the heating element can be considered one-dimensional because of the high heat-conductivity of graphite and the axial symmetry. Three characteristic sections (Fig. 1) are separated when computing the thermal losses from the outer surface. Heat transfer through the cylindrical wall that has an effective heat conductivity λ_{sh} in the radial direction is considered in section I, convective heat transfer into the closed cylindrical interlayer and radiation from the heater surface onto the surface of the shell 1 which has the temperature T_{sh} in section II, and natural convection in the closed cylindrical interlayers and radiation heat transfer from the screens 3 in section III. Taken into account in computing the thermal losses from the inner surface are radiation by the inner screen 4, the ingot 5 and heat elimination by mixed convection from the heater surface. The derivation of the heat conduction equation is analogous to the case considered in [5], which permits utilizing the results obtained there

$$c_p\rho_p(R_p^2-R_{p1}^2)\frac{\partial T_p}{\partial \tau}=\frac{\partial}{\partial z}\left[(R_p^2-R_{p1}^2)\lambda_p\frac{\partial T_p}{\partial z}\right]+\frac{I^2\nu_p}{\pi^2(R_p^2-R_{p1}^2)}-$$
$$-\xi_1 2R_p(1+R_p'^2)^{1/2}\left[2\sigma_0 n_c^2 R_{s1}(\varepsilon_p T_p^4-\varepsilon_{s1}T_{s1}^4)\int_{a_3}^{a_4}\frac{\cos\theta_1\cos\theta_2}{s_1^2}dz^*+\right.$$
$$\left.+\alpha_p(T_p-T_i)\right]-\xi_2 2R_p(1+R_p'^2)^{1/2}\left[2\sigma_0 n_c^2 R_{sh}(\varepsilon_p T_p^4-\varepsilon_{sh}T_{sh}^4)\times\right.$$
$$\left.\times\int_{c_1}^{c_2}\frac{\cos\gamma_1\cos\gamma_2}{s_4^2}dz^*+\alpha_p(T_p-T_i)\right]-\xi_3\frac{4\lambda_{sh}(T_p-T_{sh})}{\ln\frac{R_{sh}}{R_p}}(1+R_p'^2)^{1/2}- \quad (1)$$

Leningrad Institute of Precision Mechanics and Optics. Translated from Inzhenerno-Fizicheskii Zhurnal, Vol. 54, No. 2, pp. 248-256, February, 1988. Original article submitted October 8, 1986.

 0022-0841/88/5402-0176$12.50

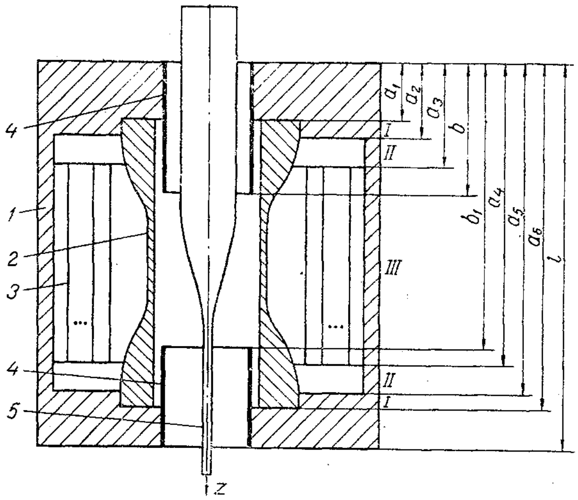

Fig. 1. Thermal model of a resistance furnace for drawing an optical fiber.

$$
-2\alpha_{p1}R_{p1}(1+R_{p1}'^2)^{1/2}(T_p-T_g)-4R_{p1}(1+R_{p1}'^2)^{1/2}\sigma_0 n_c^2\left[\xi_4 R_s(\varepsilon T_p^4-\varepsilon_s T_s^4)\int\limits_{c_3}^{c_4}\frac{\cos\varphi_1\cos\varphi_2}{s_2^2}dz^*+\right.
$$

$$
\left.+\xi_5\int\limits_{b}^{b_1}(\varepsilon_p T_p^4-\varepsilon T^4)\frac{\cos\omega_1\cos\omega_2}{s_3^2}R(1+R'^2)^{1/2}dz^*\right]. \tag{1}
$$

Here and henceforth $R' = dR/dz^*$, $R_p' = dR_p/dz$, $R_{p1}' = dR_{p1}/dz$. The first component in the right side in (1) characterizes energy transfer by heat conduction, while the second determines the power of the internal energy sources. The third component determines the surface energy sink with area element dA (Fig. 2) in the section z due to convection and radiation on the whole surface of the first screen (it is here assumed that the temperature of the first outer screen is constant and equal to T_{s1}), the fourth governs the losses due to convection and radiation directly at the shell (the section II in Fig. 1). It was assumed in the computations that $T_i = (\bar{T}_p + T_{sh})/2$, where $\bar{T}_p=\frac{1}{a_5-a_2}\int\limits_{a_2}^{a_5}T_p dz^*$. The quantity α_p was computed for the case of natural convection in a cylindrical interlayer with inner cylinder temperature greater than the outer temperature [6].

The fifth component in (1) characterizes the surface energy sink due to conductivity of the housing (section I in Fig. 1). And, finally, the last three components describe the energy sink from the inner heater surface due to convection, radiation by the inner screen and the ingot.

The angles $\psi_j = \{\omega_j, \varphi_j, \gamma_j, \theta_j\}$ are angles between the normal to the heat eliminating surface and the direction of radiation propagation (Fig. 2) and respectively equal [7]:

$$
\cos\psi_1=\frac{1}{s(1+R_{\psi1}'^2)^{1/2}}[R_{\psi2}-R_{\psi1}+iR_{\psi1}'(z-z^*)],
$$

$$
\cos\psi_2=\frac{1}{s(1+R_{\psi2}'^2)^{1/2}}[R_{\psi2}-R_{\psi1}+iR_{\psi2}'(z-z^*)],
$$

where $R_{\psi j}$ is the shape of the heat eliminating surface, and z, z* are, respectively, the coordinates along the surfaces $R_{\psi1}$ and $R_{\psi2}$ (Fig. 2);

$$
s^2=(z-z^*)^2+[R_{\psi2}(z^*)-R_{\psi1}(z)]^2;\ R_{\psi1}'=\frac{dR_{\psi1}}{dz^*};\ R_{\psi2}'=\frac{dR_{\psi2}}{dz^*},
$$

$$
j=\{1,\ 2\},\ i=\begin{cases}1, & \text{if}\ \ R_{\psi1}'<0\ \text{or}\ R_{\psi2}'<0,\\ -1, & \text{if}\ \ R_{\psi1}'>0\ \text{or}\ R_{\psi2}'>0.\end{cases}
$$

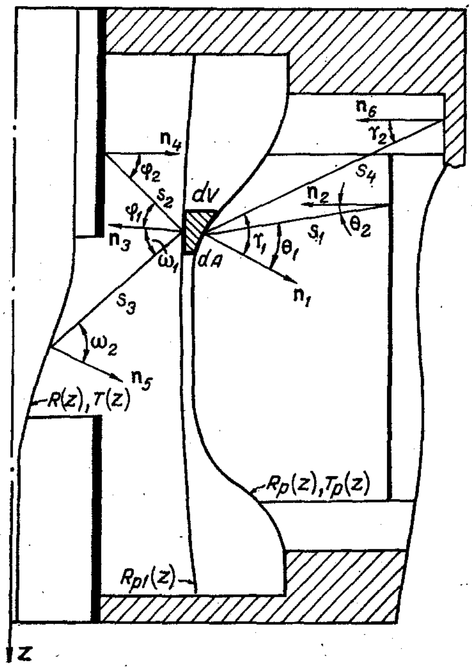

Fig. 2. To derive the heat balance equation.

The coefficients ξ_i ($i = 1, 2, \ldots, 5$) in (1) are weight factors whose magnitude is determined by the longitudinal coordinate

$$\xi_1 = \begin{cases} 1, & \text{if } a_3 < z < a_4, \\ 0 & \text{otherwise,} \end{cases} \qquad \xi_2 = \begin{cases} 1, & \text{if } a_2 < z < a_3 \text{ or } a_4 < z < a_5 \\ 0 & \text{otherwise,} \end{cases}$$

$$\xi_3 = \begin{cases} 1, & \text{if } a_1 < z < a_2 \text{ or } a_5 < z < a_6, \\ 0 & \text{otherwise,} \end{cases} \qquad \xi_4 = \begin{cases} 1, & \text{if } a_1 < z < b \text{ or } b_1 < z < a_6. \\ 0 & \text{otherwise,} \end{cases}$$

$$\xi_5 = \begin{cases} 1, & \text{if } b < z < b_1, \\ 0 & \text{otherwise.} \end{cases}$$

The integration limits c_i ($i = 1, 2, 3, 4$) are determined by the magnitude of the longitudinal coordinate

$$(c_1, c_2) = \begin{cases} (a_2, a_3), & \text{if } a_2 < z < a_3, \\ (a_4, a_5), & \text{if } a_4 < z < a_5, \end{cases}$$

$$(c_3, c_4) = \begin{cases} (a_1, b), & \text{if } a_1 < z < b, \\ (b_1, a_6), & \text{if } b_1 < z < a_6. \end{cases}$$

Let us examine in greater detail the method of determining the unknown quantities α_{p1}, T_g, T_s and T_{s1} in (1).

We consider computation of the temperature of the first outer screen. The heat flux from the whole outer heater surface onto the screen surface equals

$$Q_{p1} = 4\pi\sigma_0 R_{s1} n_c^2 \int_{a_3}^{a_4} \left[(\varepsilon_p T_p^4 - \varepsilon_{s1} T_{s1}^4) R_p (1 + R_p'^2)^{1/2} \int_{a_3}^{a_4} \frac{\cos\theta_1 \cos\theta_2}{s_1^2} dz^* \right] dz.$$

The flux from the whole surface of the first screen onto the shell surface in the presence of n screens with a constant temperature [8] is

$$Q_{об} = \frac{n_c^2 \sigma_0 F_{s1} (T_{s1}^4 - T_{sh}^4)}{\dfrac{1}{\varepsilon_{s1}} + \left(\dfrac{1}{\varepsilon_{sh}} - 1 \right) \dfrac{F_{s1}}{F_{sh}} + \sum\limits_{i=2}^{n} \left(\dfrac{2}{\varepsilon_{si}} - 1 \right) \dfrac{F_{s1}}{F_{si}}}.$$

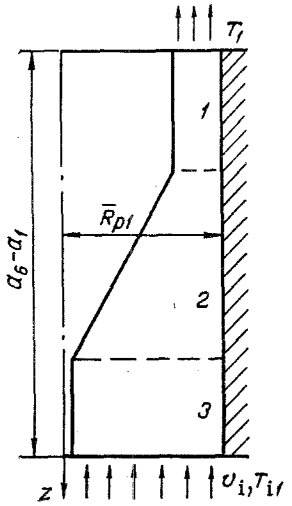

Fig. 3. To compute the external heat elimination coefficient.

In the stationary state $Q_{p1} = Q_{sh}$, from which it can be found that

$$T_{s1}^4 = \frac{2\varepsilon_p \int\limits_{a_3}^{a_4} T_p^4 \beta_1 dz + \frac{T_{sh}^4 (a_4 - a_3)}{\beta_2}}{\frac{(a_4 - a_3)}{\beta_2} + 2\varepsilon_{s1} \int\limits_{a_3}^{a_4} \beta_1 dz}, \qquad (2)$$

$$\beta_1 = R_p (1 + R_p'^2)^{1/2} \int\limits_{a_3}^{a_4} \frac{\cos\theta_1 \cos\theta_2}{s_1^2} dz^*, \quad \beta_2 = \frac{1}{\varepsilon_s} + \left(\frac{1}{\varepsilon_{sh}} - 1\right)\frac{R_{s1}}{R_{sh}} + \sum_{i=2}^{n} \frac{R_{s1}}{R_{si}} \left(\frac{2}{\varepsilon_{si}} - 1\right).$$

In the general case a computation of the temperature field of the heating element in the furnace construction with and without inner screens is of interest. A computation of the local value of the external heat elimination coefficient in the absence of inner screens will be examined below. A more general computation of α_{p1} and T_g, i.e., in the presence of inner screens or just one, will be analogous to the above-mentioned one and will not be presented because of the awkwardness of the formulas. The following assumptions were made in evaluating α_{p1} and T_g.

1. Estimates of the boundary layer thickness show that it does not fill the whole transverse section of the channel completely, therefore, the heat transfer can be considered independently for each of the walls.

2. An actual configuration of the computation domain was replaced by the domain shown in Fig. 3. Since mixed convection holds in the channel, then the local value of the Nusselt number is found from the relationship [9]

$$\mathrm{Nu}_x^3 = \mathrm{Nu}_{xc}^3 + \mathrm{Nu}_{xi}^3.$$

It is considered that mixed convection from the vertical cylinder holds in section 1 (Fig. 3), from the vertical cone in section 2, from the thin vertical filament being blown out by a longitudinal air stream from the furnace surface as from a vertical plate in section 3. The values Nu_{xc} and Nu_{xi} were found from the appropriate relationships presented in [6, 10, 11].

3. It is considered that the gas temperature along the channel length varies by a linear law from the temperature T_{i1} at the input to a certain temperature T_1 at the output:

$$T_g = \frac{T_{i1} - T_1}{a_6 - a_1} z + T_1.$$

4. Estimates show that the pressure drop in the channel is much less than one; consequently, the velocity distribution in the channel can be found from the mass conservation law with the temperature expansion of the gas taken into account [12], i.e.,

$$v_g(z) = \frac{\rho_{ri} v_i}{\rho_r(z)} \frac{\bar{R}_{p1}^2 - R_i^2}{\bar{R}_{p1}^2 - R^2(z)}.$$

Here $\bar{R}_{p1} = \frac{1}{a_6 - a_1} \int_{a_1}^{a_6} R_{p1} dz$ is the mean radius of the inner surface of the heating element, the subscript i is the value of the parameters at the channel input.

On the basis of energy conservation, the change in the internal gas energy equals the quantity of heat delivered to the channel side walls, i.e.,

$$\rho_{gi} c_{p_i} v_i (\bar{R}_{p1}^2 - R_i^2)(T_1 - T_{i1}) = 2 \int_0^{a_6 - a_1} \alpha (T - T_g) R (1 + R'^2)^{1/2} dz + 2\bar{R}_{p1} \int_0^{a_6 - a_1} \alpha_{p1} (T_p - T_g) dz. \quad (3)$$

Substituting the dependence $T_g(z)$ into (3) and solving the equation obtained for T_1, we obtain

$$T_1 = \frac{\frac{1}{2} T_{i1} \rho_{gi} c_{p_i} v_i (\bar{R}_{p1}^2 - R_i^2) + \int_0^{a_6 - a_1} \left[\alpha \left(T - \frac{T_{i1}}{a_6 - a_1} z \right) R (1 + R'^2)^{1/2} + \alpha_{p1} \bar{R}_{p1} \left(T_p - \frac{T_{i1}}{a_6 - a_1} z \right) \right] dz}{\frac{1}{2} \rho_{gi} c_{p_i} v_i (\bar{R}_{p1}^2 - R_i^2) + \int_0^{a_6 - a_1} \left(1 - \frac{z}{a_6 - a_1} \right) [\alpha R (1 + R'^2)^{1/2} + \alpha_{p1} \bar{R}_{p1}] dz}. \quad (4)$$

The gas temperature at the channel exit is computed by iteration. A certain initial approximation of the temperature T_1 is given, $T_g(z)$, $v_g(z)$ and Nu_x are computed, and the refined value of T_1 is found from (4). The iterations cease when $|T_1^i - T_1^{i+1}| < \Delta$, where i is the number of the iteration.

The equation to compute the temperature of the upper or lower inner screen is obtained analogously to (2), but gas blowing through the heating zone is taken into account by the introduction of a convective energy sink from the screen surface. We present an equation to compute the temperature of the upper screen (for the lower screen the equation is analogous):

$$T_s^4 + \frac{2\bar{\alpha}_s (b - a_1)}{\beta_3} T_s = \frac{\sigma_0 n_c^2 \left[2\varepsilon_p \int_{a_1}^{b} T_p^4 \beta_4 dz + \frac{\bar{T}^4 (b - a_1)}{\beta_5} \right] + 2\bar{\alpha}_s \bar{T}_g (b - a_1)}{\beta_3},$$

where

$$\beta_3 = n_c^2 \sigma_0 \left(\frac{b - a_1}{\beta_5} + 2\varepsilon_s \int_{a_1}^{b} \beta_4 dz \right); \quad \beta_4 = R_{p1} (1 + R_{p1}'^2)^{1/2} \int_{a_1}^{b} \frac{\cos \varphi_1 \cos \varphi_2}{s_2^2} dz^*;$$

$$\beta_5 = \frac{1}{\varepsilon_s} + \left(\frac{1}{\varepsilon} - 1 \right) \frac{R_s}{\bar{R}_p};$$

$\bar{\alpha}_s$, $\bar{T}_g$, $\bar{T}$, $\bar{R}_{p1}$ are, respectively, the mean values of α_s, T_g, T, R_{p1} in the section $(b - a_1)$; $\bar{\beta}_6 = \frac{1}{b - a_1} \int_{a_1}^{b} \beta_6 dz$; $\beta_6 = \{\alpha_s, T_g, T, R_{p1}\}$.

Let us consider selection of the boundary conditions. The heat flux delivered to the heating element endface because of heat conduction is $\lambda_p \frac{\partial T_p}{\partial z} = q_1$; a flux $q_2 = \frac{\lambda_{sh}}{d} (T_p - T_{sh})$ is transferred through a plane wall of thickness d while the flux $q_3 = \alpha_{sh}(T_{sh} - T_0)$ is dissipated in the environment. In the stationary state $q_1 = q_2 = q_3$, which permits us to obtain

$$\frac{\partial T_p}{\partial z} = \frac{\alpha_{sh}^1 \lambda_{sh}^1}{(a_1 \alpha_{sh}^1 - \lambda_{sh}^1) \lambda_p} (T_p - T_0), \quad z = a_1, \quad (5)$$

$$-\frac{\partial T_p}{\partial z}=\frac{\alpha_{sh}^2\,\lambda_{sh}^2}{[(l-a_6)\,\alpha_{sh}^2+\lambda_{sh}^2]\,\lambda_p}(T_p-T_0),\quad z=a_6. \tag{6}$$

Here λ_{sh}^1, λ_{sh}^2 is the shell conductivity in the axial direction for $z = a_1$ and $z = a_6$, respectively, α_{sh}^1 and α_{sh}^2 are the external heat elimination coefficients from the housing surface for $z = 0$ and $z = l$, the latter are determined for the case of natural convection from a horizontal plate with a heat eliminating surface turned upward and downward [6].

Thus, the heating element temperature distribution in the stationary state $\left(\frac{\partial T_p}{\partial \tau}=0\right)$ is described by (1) with the boundary conditions (5) and (6). Solution of the problem formulated was by finite differences. After approximating the initial equation, which is nonlinear, a system of nonlinear algebraic equations is obtained for whose solution some iteration process must be utilized. In this case, it is quite complicated to indicate an initial approximation of the solution such as would assure convergence of the iterations. Consequently, it is convenient to solve the problem formulated by the build-up method, i.e., the stationary heating element temperature distribution is considered the result of building up a process evolving in time. Upon giving a certain initial temperature distribution

$$T_p(z,\,\tau)=\varphi_0(z)\quad\text{for}\quad \tau=0 \tag{7}$$

it is natural to expect that the solution $T_p(z, \tau)$ will change ever more slowly with the lapse of time and go over into the equilibrium temperature distribution $T_p(z)$ in the limit as $\tau \to \infty$. Upon assigning a sufficiently small time step, T_p^i in the i-th time layer will be slightly different from T_p^{i+1} in the (i + 1)-th time layer, which will assure convergence of the iteration process when solving the system of nonlinear equations if the temperature distribution in the i-th time layer is taken as the initial approximation.

The formulated initial-boundary-value problem (1), (5)-(7) was approximated by an implicit difference scheme of second-order accuracy for equations with variable coefficients [13]. The system of nonlinear algebraic equations was solved by the Newton method [14] in each time layer. The accuracy of the iteration convergence was given in each time layer

$$\max_j\left|\frac{T_{pj}^{i+1,\,n+1}-T_{pj}^{i+1,\,n}}{T_{pj}^{i+1,\,n+1}}\right|<\Delta$$

and for the buildup

$$\max_j\left|\frac{T_{pj}^{i+1}-T_{pj}^{i}}{\varkappa}\right|<\Delta,$$

where n is the number of the iteration in the (i + 1)-th time layer, and j is the number of the node.

The computation algorithm considered above was realized in the language FORTRAN-4. It is established from computations that the iteration scheme developed turns out to converge well. To achieve steady values of the temperature, on the order of 800-1000 time steps are required while to find the solution of the nonlinear system of equations at each time layer is usually done in from 3-5 iterations by the Newton method. It is here necessary to emphasize that the computed program permits replacement of the initial data to change the furnace construction and its geometric dimensions. Namely, there is the possibility of giving, first, the absence or presence of the inner screens 4 (see Fig. 1), second, the absence or presence of any of the domains separated out earlier in Fig. 1 for the computation of the surface energy sinks or their arbitrary tracking combinations along the longitudinal coordinate, and third, arbitrary changes are possible in the shape of the inner heating element surface within the framework of axial symmetry. This permits execution of computations of the thermal mode of heating element operation for practically any resistance furnace construction for drawing optical fibers.

NOTATION

c_p, ρ_p, λ_p, specific heat, density, and heat conduction of graphite; R_p, R_{p1}, shapes of the generators of the outer and inner heating element surfaces; l, length of the furnace housing; a_i, b_j, respectively, the geometric dimensions of the furnace and the inner screen, $i = 1, 2, \ldots, 6$; $j = 1, 2$; R_s, R_{s1}, R_{sh}, R_{si}, respectively, the radii of the inner screen, the first outer screen, the shell, and the i-th outer screen; F_{s1}, F_{sh}, F_{si}, surface areas of the first screen, the shell, and the i-th screen; T_p, T_0, T, T_s, respectively, the temperatures of the heater, the surrounding air, the jet, and the temperature of the upper or lower inner screen; T_i, mean gas temperature between the heater and the shell; T_{s1}, temperature of the first outer screen; τ, time; z, longitudinal coordinate; R, shape of the jet surface generator; I, current intensity flowing through the heating element; ν_p, specific electrical resistivity of graphite; σ_0, Stefan–Boltzmann constant; n_c, refractive index of the gas being blown through the heating zone; ε, ε_p, ε_{s1}, ε_{sh}, ε_{si}, ε_s, respectively, emissivities of the ingot, heater, first outer screen, shell, i-th outer screen, inner screen; α_p, α_{sh}, external heat elimination coefficients from the external heater surface and the shell surface; α_{p1}, α, local values of the external heat elimination coefficient from the inner heater surface and jet; T_g, a function that describes the longitudinal temperature distribution of the gas blown through the heating zone; Nu_{xc}, Nu_{xs}, local values of the Nusselt number for free and forced convection; v_g, gas velocity; ρ_Γ, gas density; c_{pi}, gas specific heat at the channel inlet; Δ, error; κ, time step; s_i, distance between the heat eliminating surfaces, i = 1, 2, 3, 4; α_s, local value of the external heat elimination coefficient from the inner screen.

LITERATURE CITED

1. H.-G. Ungern, Planar and Fiber Optic Waveguides [Russian translation], Moscow (1980).
2. D. N. Payne and W. A. Gambling, Am. Ceram. Soc. Bull., 55, No. 2, 195-197 (1976).
3. Prospectus of the firm "ASTRO," Furnace Assembly HR-80, SK2465 (1980).
4. Prospectus of the firm "SENTORR." Optical Fiber Drawing Furnace 2A-100-SS, model 11A (1982).
5. V. D. Naumchik, Energy Transfer in Convective Flows [in Russian], Minsk (1985), pp. 64-67.
6. O. G. Martynenko and Yu. A. Sokovishin, Free-Convective Heat Transfer [in Russian], Minsk (1982).
7. V. N. Vasil'ev and G. N. Dul'nev, Energy Transfer in Convective Flows [in Russian], Minsk (1985), pp. 39-64.
8. V. P. Isachenko, V. A. Osipova, and A. S. Sukomel, Heat Transfer [in Russian], Moscow (1982).
9. S. W. Churchill, AIChE J., 23, No. 1, 10-16 (1976).
10. A. V. Lykov, Heat and Mass Transfer [in Russian], Moscow (1972).
11. V. R. Borovskii and V. A. Shelimanov, Heat Transfer of Small Radii Cylindrical Bodies and Their Systems [in Russian], Kiev (1985).
12. L. G. Loitsyanskii, Mechanics of Fluids and Gases [in Russian], Moscow (1973).
13. A. A. Samarskii, Theory of Difference Schemes [in Russian], Moscow (1983).
14. J. Ortega and W. Reinboldt, Iteration Methods of Solving Nonlinear Systems of Equations with Many Unknowns [Russian translation], Moscow (1975).